Chinese Chemical Letters 32 (2021) 3368–3371

Contents lists available at ScienceDirect

Chinese Chemical Letters

journal homepage: www.elsevier.com/locate/cclet

Communication

In situ growth of polydopamine on surface of covalent organic frameworks under the catalysis of acid phosphatase for dopamine detection

Fei Qu[a,b,*,1], Ziwei Guo[a,b,1], Dafeng Jiang[c], Xian-En Zhao[a,b,*]

[a] The Key Laboratory of Life-Organic Analysis, Qufu Normal University, Qufu 273165, China
[b] The Key Laboratory of Pharmaceutical Intermediates and Analysis of Natural Medicine, Qufu Normal University, Qufu 273165, China
[c] Department of Physical and Chemical Testing, Shandong Center for Disease Control and Prevention, Ji'nan 250014, China

ARTICLE INFO

Article history:
Received 11 January 2021
Received in revised form 1 April 2021
Accepted 2 April 2021
Available online 6 April 2021

Keywords:
Fluorescence
Enzyme
Polydopamine
Dopamine
Acid phosphatase

ABSTRACT

Dopamine (DA) is easy to be oxidized and polymerizes to form polydopamine (pDA) in alkaline conditions, while the synthesis is usually time-consuming (48 h). Herein, the polymerization of DA is completed with 4 h under the catalysis of acid phosphatase (ACP). The high efficiency makes the detection of DA feasibility based on the self-polymerization of DA. In this assay, pDA is grown *in situ* on the surface of covalent organic frameworks (COFs), and then the fluorescence of COFs is quenched significantly. The linear range of DA is achieved from 0.5–50 μmol/L with a detection limit of 0.16 μmol/L. The detection of DA is not interfered with uric acid, ascorbic acid, and some phenolic compounds, because these substances cannot polymerize in the presence of ACP. Moreover, benefiting from the good sensitivity and selectivity, DA has been successfully determined by this strategy in human urine samples with satisfactory recoveries.

Dopamine (3,4-dihydroxyphenylethylamine, DA) is a catecholamine neurotransmitter, which plays a significant role in both the central and peripheral nervous systems [1]. The disorder concentration of DA has been considered to be the parameter of a series of neural and metabolic diseases [2–4]. Therefore, the accurate detection of DA is of great importance. Additionally, DA can also be oxidized and polymerize to form polydopamine (pDA) under alkaline condition. For example, DA was added to the mixture of Tris-buffer (pH 8.5) and isopropyl alcohol with continuous stirring for 48 h in the dark, producing black pDA [5–7]. As well known, pDA is an effective fluorescent quencher and is utilized to detect many biomolecules [8–10]. However, there are only a few studies that report the detection of DA by the quenching property of pDA [11,12]. The reason may be that the self-polymerization of DA is time-consuming. Moreover, the detection is insensitive since DA with a low concentration is hard to self-polymerize. Thus, the establishment of a simple, feasible and high-efficiency way to monitor DA by employing pDA as the fluorescent quencher remains a challenge.

Benefiting from the advantages of nanotechnology, the special structures and optical properties of nanoscaled materials have attracted a wide attention [13,14]. Covalent organic frameworks (COFs) are a kind of popular materials, linked by covalent bonds. Schwab *et al.* reported a series of COFs by polycondensation between melamine and di- or tri-aldehydes and defined them as Schiff base networks [15]. Thanks to outstanding chemical stability, electron-rich property and unique optical feature, COFs have shown promising attention in the fields of sensing applications. For instance, through the photoinduced electron transfer (PET) mechanism, the fluorescence of COFs was quenched by electron-deficient nitroaromatic explosives including picric acid (PA) [16], 2,4,6-trinitrophenol (TNP) [17] and 2,4,6-trinitrotoluene (TNT) [18]. However, a majority of biomolecules are electron-rich. Hence, COFs are rarely used to determine biomolecules.

In this work, a fluorescent strategy for DA detection is proposed based on *in situ* growth of pDA on the surface of COFs with the aid of acid phosphatase (ACP). As shown in transmission electron microscopy (TEM) image, COFs are nearly spherical nanoparticles and the average diameter is about 45 nm (Fig. S1a in Supporting information). Comparing the Fourier transform infrared (FT-IR) spectra of terephthalaldehyde and melamine with that of COFs

* Corresponding authors at: The Key Laboratory of Life-Organic Analysis, Qufu Normal University, Qufu 273165, China.
E-mail addresses: qufei3323@163.com (F. Qu), xianenzhao@163.com (X.-E. Zhao).
[1] These authors contributed equally to this work.

https://doi.org/10.1016/j.cclet.2021.04.010

(Fig. S1b in Supporting information), the C=O stretching vibration peak of terephthalaldehyde at 1698 cm^{-1} disappears in the spectrum of COFs [15]. The two peaks at 3468.5 cm^{-1} and 3418.8 cm^{-1} of melamine are ascribed to the stretching vibration of NH_2, and the peak at 1650 cm^{-1} attributed to NH_2 deformation is also absent in the spectrum of COFs [19]. The result demonstrates that the formation of COFs depends on the dehydration reaction between the amino groups of melamine and aldehyde groups of terephthalaldehyde. Moreover, owing to the C=N vibration of triazine ring of melamine, two disparate bands at 1548 cm^{-1} and 1480 cm^{-1} appear in COFs, revealing the frameworks combined by triazine ring units. In the X-ray photoelectron spectroscopy (XPS) spectra of COFs (Figs. S1c-e in Supporting information), two peaks at 399.3 and 284.3 eV corresponding to N 1s and C 1s are observed. The spectrum of C 1s can be further fitted into four peaks. The peak at 284.6 and 285.7ev are attributed to carbon atoms in the benzene ring (C=C, C—C) of terephthalaldehyde. The peak of linkages (C—N) is located at 286.7 eV, and the peak at 287.6 eV is assigned to the carbon atom in the triazine ring (C=N) of melamine [20]. These results reveal the successful crosslinking between the monomers after pyrolysis [21]. Furthermore, the N 1s can be grouped into two peaks at 398.6 and 399.8 ev corresponding to nitrogen atoms in the triazine ring (C=N) of melamine and amine (NH) moieties of linkages, respectively [22]. The spectra of XPS confirm the formation of COFs, and the functional groups of COFs are triazine rings, benzene rings and aminol groups. Besides, the elemental analysis suggests that COFs are mainly constituted of C, H and N elements, and their content are 63.44%, 4.8% and 31.72%, respectively. It further proves that COFs are composed of light elements. Moreover, COFs display a blue emission centered at 470 nm with the maximum excitation wavelength at 370 nm (Fig. S1f in Supporting information). According to the reported works, the triazine ring units associated with the π-π^* electronic transitions are the main reason for the luminescence of COFs [20,23]. COFs also show a good stability, and their fluorescence can maintain a high level at least one month and in a wide pH range (Fig. S2 in Supporting information).

As well known, ACP can cleave a phosphate group from related substrates. However, the catalytic effect of ACP on DA polymerization is different from it, because there is no phosphate group in DA. The UV–vis characterization of DA polymerization is used to compare the ACP-mediated reaction (PBS buffer, pH 7.0) with pH-induced one (Tris-Buffer, pH 8.5). As illustrated in Figs. 1a and b, the peak at 280 nm is attributed to the π-π^* electronic transitions of DA [24], and ACP displays an absorbance peak at 225 nm due to the nature of protein absorption. Especially, the shoulder peak at around 475 nm is developed at first 5 min in both ACP-mediated and pH-induced polymerization, and it is the n-π^* electronic transitions of dopaquinone [25]. Dopaquinone is the initial oxidation product of DA. Then, another should peak at 320 nm can be distinguished after 45 min in ACP-mediated reaction and 4 h in pH-induced one. It is ascribed to the formation of 5,6-dihydroxyindole *via* intramolecular cyclization [26]. 5,6-dihydroxyindole is further oxidized into 5,6-indolequinone. Subsequently, both integrate into dimers or trimers, then polymerization of DA [27]. A useful distinction can be drawn between these two ways. The absorbance at 475 nm changes significantly in pH-induced polymerization, revealing the formation of large amount of dopaquinone. However, the absorbance variation at 320 nm is clear in ACP-mediated reaction, so 5,6-dihydroxyindole or 5,6-indolequinone is the main intermediate. It is speculated that the catalysis of ACP accelerates the conversion from DA to 5,6-dihydroxyindole or 5,6-indolequinone. Therefore, ACP-mediated oxidation shortens the time of pDA formation, implying higher efficiency. Similarly, the study of Pan's group also suggested the reducing agent suppressed the polymerization of DA catalyzed by ACP, but the inhibitors of ACP had no such effect [28]. It means that the catalysis of ACP in DA polymerization is related to the oxidation. Herein, our assay also supports this view.

For another, the mixture color changes from colorless to brown and then to black after 4 h in ACP-mediated oxidation or 48 h in pH-induced one (inset of Fig. 1), also indicating the complete formation of pDA. As shown in the Scanning electron microscope (SEM) images (Figs. 1c and d), there are some regular-shaped pDA and amounts of irregular agglomerates in ACP-mediated oxidation. However, the obtained pDA nanoparticles are all spherical in pH-induced polymerization. The reason may be that some fragments have not agglomerate to form regular sphere in the short time of ACP-mediated oxidation. Besides, particle size (about 500 nm), functional groups, and charges of the particles formed in these two ways are similar (Figs. S3a and b in Supporting information). On the above discussions, ACP-mediated oxidation provides an efficient choice for the preparation of pDA. Other enzymes and protein cannot catalyze the oxidation and polymerization of DA in neutral medium (Fig. S4 in Supporting information), suggesting the high specificity of ACP for DA in the polymerization.

Based on *in situ* growth of pDA on the surface of COFs, the emission of COFs is quenched significantly (Fig. 2a), and the color of the solution changes to black, which can be distinguished by bare eyes. However, when DA or ACP is added alone, no obvious change in the fluorescence intensity is observed, and the solution remains transparent under the daylight. Subsequently, the quenching mechanism has been investigated. In the process of ACP-mediated oxidation, the initial oxidation product of DA is dopaquinone [29]. However, dopaquinone makes a negligible

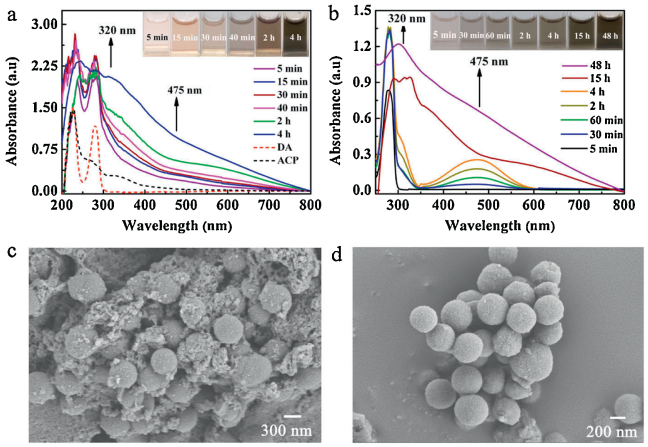

Fig. 1. UV–vis characterization of DA polymerization in ACP-mediated reaction (a) and in pH-induced one (b) with different reaction time. SEM images of pDA formed after 4 h in ACP-mediated reaction (c) and pDA formed after 48 h in pH-induced polymerization (d).

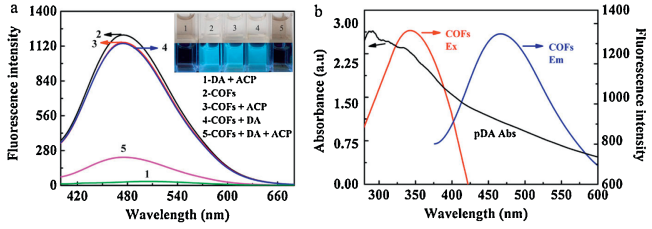

Fig. 2. (a) Fluorescence spectrum of the mixture of DA and ACP (curve 1); the fluorescence spectra of COFs in the absence (curve 2) and presence of ACP (curve 3), DA (curve 4), and the mixture containing DA and ACP (curve 5), and the corresponding photographs (inset). (b) Comparison of the UV–vis absorption spectrum of pDA with fluorescence excitation and emission spectra of COFs.

effect on the fluorescence of COFs (Fig. S5b in Supporting information). Hence, the fluorescence quenching of COFs is ascribed to pDA rather than dopaquinone. Additionally, it is observed that the absorption spectrum of pDA overlaps well with both of the excitation and emission spectra of COFs (Fig. 2b). The result signifies that the quenching mechanism may be Forster resonance energy transfer (FRET) or inner filter effect (IFE). After incubation with DA and ACP, the fluorescence decay of COFs changes from 12.3416 ns to 9.3742 ns (Fig. S6 in Supporting information). The FRET efficiency is evaluated by the Eq. 1 [30]:

$$E = 1 - \tau/\tau_0 \quad (1)$$

where E is the FRET efficiency, τ (τ = 9.3742 ns) and τ_0 (τ_0 =12.3416 ns) are the fluorescence lifetimes of the COFs in the presence and absence of DA and ACP. The calculated FRET efficiency is 24%. Subsequently, the quenching efficiency for IFE of pDA on the fluorescence of COFs is further studied according to Eq. 2 [31]:

$$\mathrm{CF} = \frac{F_{\mathrm{cor}}}{F_{\mathrm{obsd}}} = \frac{2.3\ dA_{\mathrm{ex}}}{1 - 10^{-dA_{\mathrm{ex}}}}\ 10^{gA_{\mathrm{em}}}\frac{2.3\ sA_{\mathrm{em}}}{1 - 10^{-sA_{\mathrm{em}}}} \quad (2)$$

where CF represents the correction factor; F_{obsd} stands for the maximum fluorescence intensity of COFs with addition of DA at 470 nm and F_{cor} is corrected fluorescence intensity by removing the IFE from F_{obsd}; A_{ex} and A_{em} refer to the absorbance of COFs with the addition of DA at 370 and 470 nm, respectively; d represents the width of the cuvette (1.00 cm); g denotes the distance between the edge of the excitation beam and the edge of the cuvette (0.40 cm) and s is the thickness of excitation beam (0.10 cm). In order to obtain more precise measurements, the value of CF should not exceed 3. As shown in Table S1 (Supporting information), the CF of IFE and relevant parameters with addition of different concentrations of DA are calculated at different temperatures. The corrected suppressed efficiency (E%) of pDA is obtained on the basis of the Eqs. 3 and 4:

$$E_{\mathrm{obsd}} = 1 - F_{\mathrm{obsd}}/F_{\mathrm{obsd},0} \quad (3)$$

$$E_{\mathrm{cor}} = 1 - F_{\mathrm{cor}}/F_{\mathrm{cor},0} \quad (4)$$

where $F_{\mathrm{obsd},0}$ or $F_{\mathrm{cor},0}$ represents the observed or the corrected fluorescence intensity of COFs in the absence of DA and ACP. As depicted in Fig. S7 (Supporting information), the quenching effect attributed to IFE at 298 K is 22% after calculation. Almost 46% of quenching effect results from FRET and IFE, revealing other quenching mechanism also coexisting.

Then, Stern-Volmer equation [32] is employed to evaluate the role of static quenching effect (SQE) or dynamic quenching effect (DQE) in fluorescence suppression (Eq. 5).

$$\frac{F_0}{F} = 1 + K_{\mathrm{SV}}[\mathrm{Q}] = 1 + K_{\mathrm{q}}\tau_0[\mathrm{Q}] \quad (5)$$

F_0 and F denote the fluorescence intensities of COFs before and after the addition of quencher. Considering IFE, $F_{\mathrm{cor},0}$ and F_{cor} should take place of the F_0 and F. K_{SV} represents the Stern-Volmer quenching constant and [Q] is the concentration of DA; K_{q} refers the quenching rate constant and τ_0 is the fluorescence lifetime of free COFs (τ_0 = 12.3416 ns). As presented in Fig. S8 (Supporting information), the corrected fluorescence intensity ratios increase linearly with the concentration of DA at different temperatures, indicating that the existing quenching mechanism is SQE or DQE [33].

Furthermore, DQE and SQE can be distinguished by their dependence on temperature. In DQE process, the fluorescence quenching is due to collision between the excited-state fluorophore and the quencher, leading to non-radiative transitions to the ground state. Thus, the higher temperature accelerates the collision, resulting in the increase in the K_{SV} [34]. For SQE, the fluorescence quenching is due to the formation of nonfluorescent ground-state complex between the fluorophore and quencher. The higher temperature leads to the lower stability of the complex, so higher temperature is responsible for a smaller value of K_{SV}. The obtained K_{SV} values at 298, 303 and 308 K are 2.019×10^4, 2.267×10^4 and 2.523×10^4 L/mol, respectively (Fig. S8 in Supporting information). The K_{SV} value is proportional to the increasing temperature, indicating that the fluorescence quenching of COFs by pDA is mainly ascribed to DQE. Additionally, fluorescence lifetime is another important difference in the SQE and DQE. It decreases in the DQE, but it remains constant for SQE with the addition of the quencher [35]. In this assay, the fluorescence lifetime of COFs declines from 12.3416 ns to 9.3742 ns after incubation with DA and ACP, suggesting that the fluorescence quenching is due to DQE. The above proofs indicate that the fluorescence quenching of COFs by pDA is ascribed to the combination of FRET, IFE and DQE.

In order to obtain a sensitive response to DA, several experimental conditions are optimized (Fig. S9 in Supporting information) and detailed description are given in the Supplementary information. Under the optimal conditions, the fluorescence of COFs at 470 nm is quenched linearly with the concentration of DA increasing from 0.5 μmol/L to 50 μmol/L (Fig. 3). The LOD is 0.16 μmol/L which is calculated based on $3\sigma/K$, where σ is the standard deviation of the blank sample and K is the slope of the calibration curve.

A series of interfering substances are tested to assess the selectivity of this method for DA, including 16 kinds of amino acids, bisphenol A, phenol, resorcinol, phloroglucinol, 2,4-chlorophenol, bovine serum albumin, uric acid (UA), ascorbic acid (AA). As depicted in Fig. S10 (Supporting information), it is obvious that all species do not influence on the fluorescence intensity of COFs without or with addition of DA in the presence of ACP. Especially, UA and AA, as the common coexistence substances in human urine, cannot polymerize with addition of ACP, so they do not interfere with the detection of DA. Furthermore, phenolic compounds are not oxidized under the catalysis of ACP due to absence of O-dihydroxy group. Therefore, the proposed probe shows a high selectivity toward DA.

Moreover, this method is compared with other strategies for DA detection in Table S2 (Supporting information). At present, the predominant methods for determining DA are electrochemical and fluorescent analysis. In electrochemical analysis, the current change generated by $2e/2H^+$ redox reaction relies on the concentration of DA [36]. The sensitivity of electrochemistry is good, but the selectivity is not satisfactory. In real sample detection, some coexistence substances, such as UA and AA, interferes with the DA detection because their oxidation potentials are close to DA [37]. Furthermore, fluorescent detection of DA is

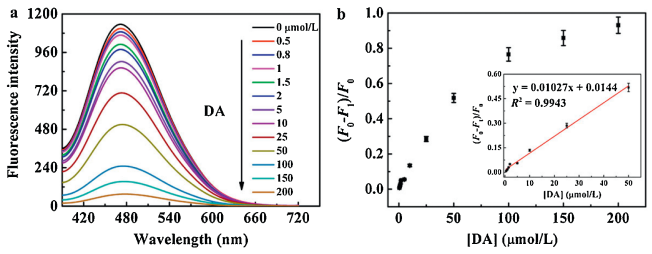

Fig. 3. (a) Fluorescence spectra of COFs in the presence of ACP and various concentrations of DA. (b) The corresponding calibration curve and linear range (inset) of DA. F_0 and F_1 represent the fluorescence intensity of COFs before and after addition of DA in the presence of ACP.

Table 1
Detection of DA in urine samples.

DA Added (μmol/L)	Proposed method			ELISA Kit		
	Found (μmol/L)	Recovery (%)	RSD	Found (μmol/L)	Recovery (%)	RSD (n = 3,%)
0	1.61	–	–	1.68	–	–
5	6.64	100.60	2.5	6.59	98.21	2.0
10	11.73	101.20	2.3	11.83	101.50	1.4
30	31.70	100.30	3.0	31.87	100.60	1.7

usually realized by the oxidation of DA to dopaquinone. The strong electron-withdrawing ability of dopaquinone makes it a good quencher for various probes. However, tyrosine and some phenolic substrates are also oxidized into quinones [29], so these substances may also interfere with the detection of DA. In this work, a series of evidences show that ACP accelerates the polymerization of DA, but it cannot catalyze the oxidation of UA, AA and other phenolic compounds. The results reveal that the selectivity of this new method is superior to that of electrochemistry and other fluorescent methods, and the sensitivity is not inferior to other ways.

The precision and reproducibility of this method for the detection of DA are studied. The intra-day and inter-day precisions of the assay are determined by estimating the corresponding response 3 times on the same day and on 3 different days over a period of one week. As shown in Table S3 (Supporting information), the relative standard deviation (RSD) of intra-day precision (CV%) ranges from 1.2% to 2.3%, and the RSD of inter-day (CV%) is in the range from 2.1%–3.9%, suggesting a good stability and precision of this method. Subsequently, the proposed method is applied to the determination of DA in human urine samples. The detected concentration of DA in the 2-fold diluted human urine sample is about 0.805 μmol/L, which is corresponding to 1.61 μmol/L of DA in the urine sample (without dilution). The result is in agreement with the normal range of 0.3–2.18 μmol/L [38]. Then, the standard DA solutions with three different concentrations are spiked into urine samples, and the recoveries in the range of 100.3%–101.2% are satisfactory (Table 1). ELISA is chosen as a reference method for DA detection. There is no significant difference between the results of ELISA and those of this strategy, demonstrating the reliability and accuracy of this proposed strategy for determination of DA. Besides, the detection of DA is also performed in cell lysate (Table S4 in Supporting information), and the satisfactory recoveries are obtained. Hence, this method has the potential for applications in complex biological samples.

In summary, this assay provides the first case that the detection of DA is realized by employing *in situ* growth of pDA on the surface of COFs under the catalysis of ACP. The advantages of this strategy lie on two aspects. One is that ACP-mediated oxidation shortens the time remarkably for the polymerization of DA, so it provides a feasible strategy for DA detection. The other one is the good selectivity toward DA because the common coexistence substances cannot be oxidized under the catalysis of ACP. Thus, the findings not only have the potential to monitor DA in clinical diagnosis but also expand the applications of COFs.

Compliance with ethical standards

The human urine sample experiments were performed with the approval of the Guidelines for Ethical Committee, Qufu Normal University. All urine samples were from health volunteers with their informed consent. All studies were approved by Ethical Committee, Qufu Normal University.

Declaration of competing interest

The authors declare that they have no known competing financial interests or personal relationships that could have appeared to influence the work reported in this paper.

Acknowledgments

This work was supported by the Natural Science Foundation of Shandong Province, China (No. ZR2019QB010), National Natural Science Foundation of China (Nos. 21705095, 21775088) and the Scientific Research Foundation of Qufu Normal University (No. BS D20130117).

Appendix A. Supplementary data

Supplementary material related to this article can be found, in the online version, at doi:https://doi.org/10.1016/j.cclet.2021.04.010.

References

[1] L. Xie, Y. Zhang, F. Gao, et al., Chin. Chem. Lett. 28 (2017) 41–48.
[2] J.T. Del Bonis, O. Donnell, A. Thakrar, J.W. Hirschberg, et al., ACS Chem. Neurosci. 9 (2018) 849–857.
[3] B. Yu, H. Yuan, Y. Yang, et al., Chin. Chem. Lett. 25 (2014) 523–528.
[4] R.V.M. Manalo, Med. Hypotheses 32 (2019) 109377.
[5] S. Xu, Y. Nie, L. Jiang, et al., Anal. Chem. 90 (2018) 4039–4045.
[6] Y. Liang, J. Wei, Y.X. Hu, et al., Nanoscale 9 (2017) 5323–5328.
[7] M. Wang, S. Wang, D. Su, et al., Anal. Chim. Acta 1035 (2018) 184–191.
[8] M. Yang, H. Zhou, Y. Zhang, et al., Microchim. Acta 185 (2018) 132.
[9] Y. Jiang, Y. Tang, P. Miao, Nanoscale 11 (2019) 8119–8123.
[10] Y. Cen, W. Deng, R. Yu, et al., Talanta 180 (2018) 271–276.
[11] J. Peng, C. Han, J. Ling, et al., Luminescence 33 (2018) 168–173.
[12] S. Weng, D. Liang, H. Qiu, et al., Sens. Actuators B: Chem. 221 (2015) 7–14.
[13] L. Liu, S. Zhu, J. Sun, et al., Chin. Chem. Lett. 32 (2021) 906–909.
[14] S. Zhao, M. Golestani, A. Penesyan, et al., Chin. Chem. Lett. 31 (2020) 851–854.
[15] M.G. Schwab, B. Fassbender, H.W. Spiess, et al., J. Am. Chem. Soc. 131 (2009) 7216–7217.
[16] Y. Zhang, T. Zhan, T. Zhou, et al., Chem. Commun. 52 (2016) 7588–7591.
[17] G. Das, B.P. Biswal, S. Kandambeth, et al., Chem. Sci. 6 (2015) 3931.
[18] J. Liu, S. Yang, F. Li, et al., J. Mater. Chem. A 3 (2015) 10069.
[19] R. Xue, H. Guo, T. Wang, et al., Mater. Lett. 209 (2017) 171–174.
[20] G. Yang, H. Han, C. Du, et al., Polymer 51 (2010) 6193–6202.
[21] J. Liu, Y. Nan, X. Chang, et al., Int. J. Hydrogen Energy 42 (2017) 10802–10812.
[22] X. Lin, X. Li, F. Li, et al., J. Mater. Chem. A 4 (2016) 6505–6512.
[23] Y. Zhao, Z. Liu, W. Chu, et al., Adv. Mater. 20 (2008) 1777–1781.
[24] K. Cheng, M. Li, S. Zhang, et al., Colloids Surf. A 582 (2019) 123846.
[25] X. Zhao, C. Lei, Y. Wang, et al., RSC Adv. 1 (2016) 72670–72675.
[26] B.P. Lee, J.L. Dalsin, P.B. Messersmith, Biomacromolecules 3 (2002) 1038–1047.
[27] C. Zhang, M. Ma, T. Chen, et al., ACS Appl. Mater. Interfaces 9 (2017) 34356–34366.
[28] J. Pan, C. Miao, Y. Chen, et al., Chem. Pharm. Bull. 68 (2020) 628–634.
[29] Y. Teng, X. Jia, J. Li, et al., Anal. Chem. 87 (2015) 4897–4902.
[30] V. Biju, T. Itoh, Y. Baba, et al., J. Phys. Chem. B 110 (2006) 26068–26074.
[31] W. Zhai, C. Wang, P. Yu, et al., Anal. Chem. 86 (2014) 12206–12213.
[32] M.I. Halawa, F. Wu, M.N. Zafar, et al., J. Mater. Chem. B 16 (2020) 3542–3549.
[33] S. Xavier, G. Siva, J. Annaraj, et al., Sens. Actuators B: Chem. 259 (2018) 1133–1143.
[34] X. Wang, X.B. Li, W.F. Chen, et al., Spectrochim. Acta A. 198 (2018) 1–6.
[35] F. Qu, Y.R. Ding, X.X. Lv, et al., Anal. Bioanal. Chem. 411 (2019) 3979–3988.
[36] K. Jackowska, P. Krysinski, Anal. Bioanal. Chem. 405 (2013) 3753–3771.
[37] X. Tan, T. Mu, Sheng Wang, et al., Analyst 146 (2021) 262–269.
[38] A. Basolo, T. Ando, T. Hollstein, et al., Obesity 28 (2020) 953–961.